Evolution of Fermi Level Crossings versus H Coverage on W(110)

Eli Rotenberg* and S. D. Kevan

Department of Physics, University of Oregon, Eugene, Oregon 97403

(Received 27 June 1997)

Two-dimensional Fermi contours of clean and hydrogen-induced surface electronic states have been systematically measured vs coverage of H on W(110) using angle-resolved photoemission. We observe a new pair of spin-orbit-interaction-split surface states, whose splitting grows systematically with hydrogen coverage and whose Fermi contours are strongly nested due to their opposing curvatures. Momentum-dependent electronic transitions between these states drive two previously observed anomalous behaviors: The phonon anomalies along $\overline{\Gamma H}$ and $\overline{\Gamma S}$ observed with inelastic helium scattering and electron energy loss spectroscopy, and the shifted-upper-layer reconstruction observed by low-energy electron diffraction for coverages greater than 0.5 monolayer. [S0031-9007(98)05539-2]

PACS numbers: 73.20.At, 63.20.Kr, 73.20.Mf

Recently, the adsorption of hydrogen on W(110) has received detailed attention due to a series of fascinating experimental observations of both the static and dynamical properties of this system. First, anomalous phonon softenings have been observed using both helium atom scattering (HAS) [1] and electron energy loss spectroscopy (EELS) [2,3]. Recent calculations [4–8] have suggested that these are Kohn anomalies which result from strong coupling between phonon and electron-hole pair excitations. This condition results when strong Fermi surface "nesting" creates a one-dimensional-like singularity in the electronic screening response [9]. These calculations, however, were in contradiction with experimental photoemission measurements [10], which predicted much larger nesting vectors than could account for the HAS or EELS data. Second, asymmetrical low-energy electron diffraction (LEED) patterns [11] suggested a dramatic surface reconstruction, with onset at a coverage $\theta_{\mathrm{H}} \approx 0.5$ monolayers (ML), consisting of a uniform lateral displacement of the uppermost W layer along $[\bar{1}10]$. This was supported by measurements [12] which showed the low-coverage hydrogen diffusion anisotropy to be lifted at $\theta_{\mathrm{H}} = 0.5$ ML. Additional, although less direct, evidence for a reconstruction comes from the observed discontinuities in the work function, surface Fermi wave vector [10], and the W $4f$ surface core level shift [13] at $\theta_{\mathrm{H}} \approx 0.5$ ML.

In this Letter, we examine whether these structural changes—dynamic (phonon anomalies) and static (shifted layer reconstruction)—are driven by momentum transfer between phonons and electronic states at the Fermi level. The momentum dependence of these states over the surface Brillouin zone (SBZ) is determined systematically as a function of θ_{H} and parallel momentum $\mathbf{k}_{||}$ using high-energy and high-angular resolution photoemission spectroscopy (ARPES). We infer that both types of structural change are, in fact, driven by electronic transitions at the Fermi level. Our experimental Fermi contour measurements are quantitatively and qualitatively in disagreement with recent calculations [4–8,14] as well as previous experiment [10]. This is due to an important effect, neglected in most theoretical treatments, namely, spin-orbit interaction, which splits the relevant surface state. This splitting increases systematically with hydrogen coverage, and fully reconciles the HAS and EELS phonon anomalies with ARPES, so that although the phonon softening may still be a Kohn anomaly, the associated nesting vector is not between the same states considered in the theoretical calculations. We also show that at critical coverage $\theta_{\mathrm{c}} \approx 0.6$ ML, roughly the same coverage as for the shifted layer reconstruction [11], the Fermi contours undergo a topological change. We propose the altered electronic response at this critical coverage to be a possible driving mechanism for this reconstruction.

A W(110) crystal was cleaned with techniques described elsewhere [10]. Hydrogen coverage was calibrated according to the W $4f$ surface core-level shifts [13]. Angle-resolved photoemission spectroscopy was performed *in situ* near room temperature using undulator-generated soft x rays at beam line 7 of the Advanced Light Source [15]. The hemispherical electron spectrometer's axis and the photon beam were coplanar with and kept at fixed angles (90° and 30°, respectively) to the sample's polar rotation axis (θ). The angular resolution was better than 0.75°, while the total instrumental resolution was $\sim$100 meV. The resulting momentum resolution (statistical error in k) of the measured Fermi wave vectors was $\sim$0.02 Å^{-1}. Fermi contour maps were obtained by fixing our detector's energy window on the Fermi level and rotating the sample. The systematic error associated with using a finite energy window was only of the order 0.02 Å^{-1}, the amount depending on the rate of dispersion through E_{F}. This systematic error always makes electron (hole) orbits look smaller (larger) by roughly this radius. For qualitative observations of Fermi surface topology, this systematic uncertainty is unimportant. For quantitative measurements, the Fermi crossings were always extrapolated from valence band spectra. Conversion of transitions with binding

energy E from emission angle θ to k-space coordinates was through $k_{||} = 0.5124\sqrt{h\nu - E - \Phi_W}\sin\theta$, where $\Phi_W = 5.9$ eV. Surface states were distinguished from bulk states by checking the independence of their binding energies with $k_\perp$, the affect on them by adsorbates, and whether they exist within gaps in the projection of bulk states onto (110).

Figure 1 shows typical Fermi contour maps for (a) clean, (b) ~0.5 ML, and (c) 1.0 ML hydrogen, for $h\nu = 100.0$ eV. Surface Fermi contours, highlighted with lines as guides to the eye, are labeled with letters for those characteristic of bare W and which disappear with increasing coverage, and with numbers for those which evolve topologically with coverage without disappearing. (The brightest features near the middles of these images are bulk transitions.) The data shown in Fig. 1 were acquired for ~1340 points over a 134° azimuthal sector and symmetrized. For saturation coverage the measurement was also carried out over a 270° sector, and the result was virtually identical to the mirror-symmetrized data, except for minor intensity variations due to the violation of strict mirror-plane symmetry in our geometry. For these room temperature measurements, the surface H atoms form a disordered layer at coverages $0 < \theta_H < 1$, accounting for a reduced sharpness and an increased diffuse background evident for intermediate coverages as in Fig. 1(b).

By comparing Figs. 1(a)–1(c), as well as by examining data for intermediate coverages not presented here, we come to some of the same qualitative conclusions regarding the Fermi contour evolution as do Gaylord *et al.* [10]: (i) Orbits A–C surrounding $\overline{S}$, $\overline{\Gamma}$, and $\overline{N}$, respectively, are quenched at 0.5 ML (highlighted as ellipses in Fig. 1) and (ii) the surface Fermi contour (labeled 1) surrounding the projection of the bulk electron jack expands, leading to a new closed, oval-shaped hole orbit surrounding $\overline{S}$. Missed in the previous experiment [10] and calculations [4,6–8] is a new surface resonance (labeled 2) which begins very close to the edge of the projected bulk states, and which becomes a proper surface state as it expands with hydrogen coverage away from the bulk states. By saturation, orbit 2 has expanded to the point where it appears similar to orbit 1 of the clean surface. Even disregarding orbit 2, the previous experiment predicts a much smaller orbit 1 than here or in theory. Also missed in the previous experiment is the noticeable shrinkage of orbits A–C before they have faded entirely, a point we will return to in the second half of the paper. We ascribe these experimental differences to systematic improvements implemented in the present study: (a) Electrons with a higher kinetic energy as used here have simpler, free-electron final states and are also less susceptible to stray fields (perhaps explaining the "egg-shaped" orbit 1 seen in Gaylord *et al.*), and (b) we now probe many more k points owing to much higher photon flux.

We now address quantitatively whether the phonon anomalies, observed at momenta $\mathbf{Q}_{c1}$ along $\overline{\Gamma H}$ and $\mathbf{Q}_{c2}$ along $\overline{\Gamma S}$ in Fig. 1(c), are generated by electronic transitions. If these vectors span nested Fermi contours, then these anomalies are of the Kohn type. Figure 2(a) shows valence band measurements (binding energy vs momentum) along $\mathbf{Q}_{c1}$; two sharp, parabolic surface bands which cross the Fermi level are observed. From these crossings, three possible nesting vectors, $\mathbf{Q}_{11}$, $\mathbf{Q}_{12}$, and $\mathbf{Q}_{22}$ for transitions between states $1 \leftrightarrow 1$, $1 \leftrightarrow 2$, and $2 \leftrightarrow 2$, were accurately determined as shown in the figure. These are to be compared with $Q_{c1} = 0.93$ Å^{-1} [1–3] determined from the phonon measurements. Figure 2(b) shows the topology of the related surface Fermi contours within the wedge at the top of Fig. 1(c). (Apart from the surface states 1–3 indicated, the remaining bright intensity near the center and upper corners is due to unimportant bulk transitions.) Figure 2(b) also shows calculated Fermi crossings from

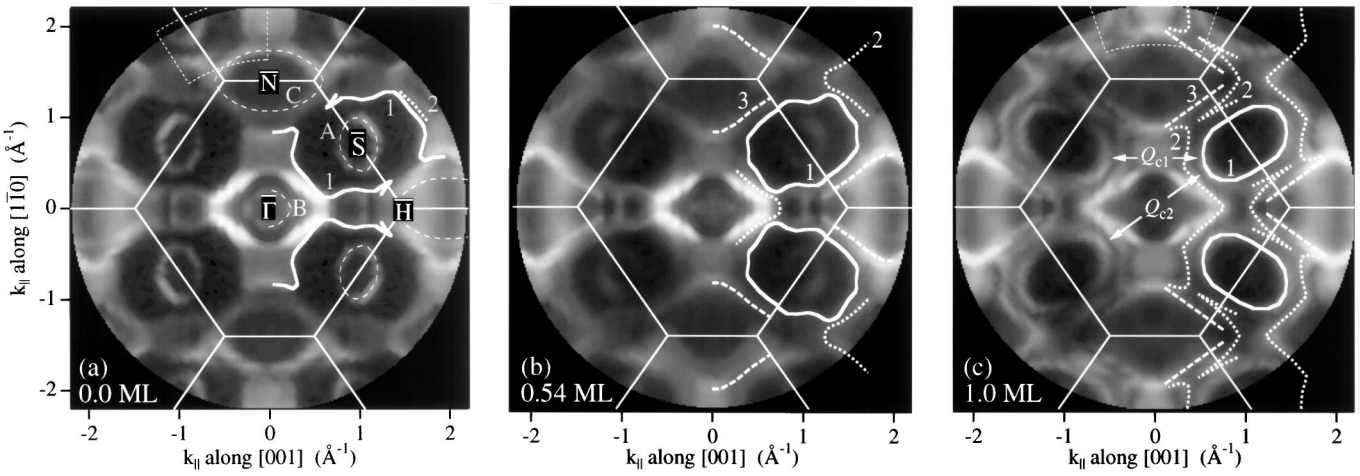

FIG. 1. Fermi photoelectron intensity for (a) clean, (b) 0.54 ML, and (c) 1 ML H on W(110), with surface orbits indicated with lines as guides to the eye. Orbits A–C are associated with bare W atoms and disappear with increasing H coverage. Orbits 1 and 2 are present on the clean surface and evolve smoothly with hydrogen coverage. Orbit 3, perhaps barely seen for the clean surface, becomes monotonically stronger with H coverage.

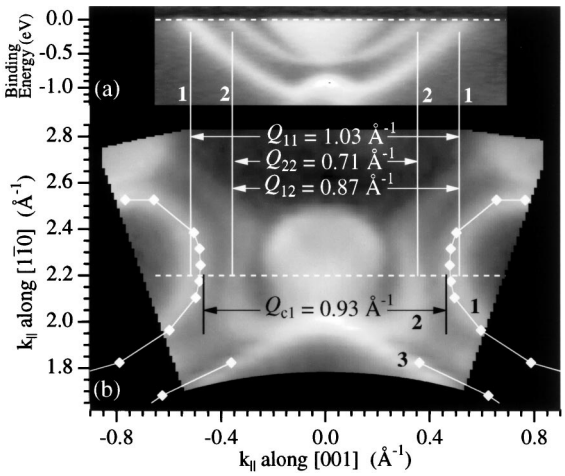

FIG. 2. Photoelectron intensity for (a) valence band and (b) Fermi level for the wedge shown in the upper part of Fig. 1(c). The spectra shown in (a) are acquired along the dashed line in (b); the various coupling vectors in $\mathbf{Q}_{ij}$ are discussed in the text. The diamonds show the calculation from Ref. [6].

Kohler *et al.* [6] (diamonds); similar results have been obtained by others [4,5,8]. All of the calculations predict only a single, closed orbit which lies somewhere between our observed orbits 1 and 2, with those of Kohler *et al.* the closest in size to orbit 1. Since the calculated orbits are artificially larger than orbit 1, these authors find a nesting vector between these orbits which is by chance in good agreement with Q_{c1}. However, considering the reduced size of orbit 1 we obtain experimentally, we conclude that the Kohn anomaly is actually between the distinct surface bands $1 \leftrightarrow 2$; this conclusion is supported not only because of the better agreement between Q_{12} and Q_{c1} but also for the reasons discussed below.

The topology of the orbits in Fig. 2(b) is an important aspect of the Kohn anomaly. The greater the degree of nesting (i.e., parallelism of the orbits), the greater the singularity in the electron-hole response function and hence the stronger the Kohn anomaly. Transitions from $1 \leftrightarrow 1$ and $2 \leftrightarrow 2$ across the SBZ are between Fermi contours of opposite curvature; hence there should be only weak singularities in the response function at the wave vectors $\mathbf{Q}_{11}$ and $\mathbf{Q}_{22}$. On the other hand, the nesting is enhanced for transition $1 \leftrightarrow 2$ since from one side to the other of the SBZ, orbits 1 and 2 have parallel curvatures (orbits 1 and 2 on the *same* side of the SBZ form an hourglass locally near the dashed line), which can also cause an anomaly [16]. The resulting singularity in the response function is further enhanced by a factor of 2 since there are two identical transitions. Therefore, we find considerably greater nesting for transition $1 \leftrightarrow 2$ than for the transition $1 \leftrightarrow 1$. Although we did not analyze the second anomaly [$\mathbf{Q}_{c2}$ in Fig. 1(c)] in as great a detail, inspection of Fig. 1(c) shows that this transition is also between orbits $1 \leftrightarrow 2$ rather than between orbits $1 \leftrightarrow 1$.

Why is orbit 2 missing from the calculations? Perhaps some interaction, not accounted for in the theory, splits the calculated orbit into the two orbits 1 and 2 seen in the experiment. The most likely possibility, already predicted to split surface states on W(001) [17], is spin-orbit coupling, which was recently observed to split the *sp*-derived surface band in Au(111) [18]. Further evidence that spin-orbit coupling or another relativistic effect is involved is provided by similar measurements for clean and hydrogen-saturated Mo(110), for which this effect should be less important. We have found no such splitting in that system [19], in agreement with theoretical calculations for H/Mo(110) [20]. A detailed theoretical analysis discerning the relative spin ordering of orbits 1 and 2 would thus be very desirable, as would spin-resolved photoemission studies. That orbits 1 and 2 are indeed spin-orbit split strengthens the argument that the transition responsible for the Kohn anomaly must be $1 \leftrightarrow 2$ and not $1 \leftrightarrow 1$ or $2 \leftrightarrow 2$. The latter transitions would necessitate a spin flip due to mirror-plane symmetry, and as the electron-phonon interaction does not couple opposite spins, these transitions would be forbidden.

We now address whether the evolution of the Fermi contours with hydrogen coverage θ_H can be related to the proposed rigid shift of the upper W layer at critical coverage $\theta_c = 0.5$ ML [11]. Figure 3 presents a sequence of scans taken within the wedge at the top of Fig. 1(a) for increasing hydrogen coverages $0 \leq \theta_H \leq 1$ ML. We find that somewhere between frames 3(c) and 3(d), orbit 1 changes topology from two disconnected contours to a closed orbit; therefore we assign θ_c to occur between frames 3(c) and 3(d), so that $\theta_c \approx 0.60 \pm 0.05$ ML. This coverage also concides with the disappearance of the closed orbits A–C in Fig. 1(a), which is reasonable since at $\theta_H = 0.5$ ML, each W atom is coordinated on the average to one hydrogen atom, saturating the dangling bonds from which states A–C are derived. From the clean surface 3(a) to frame 3(c), orbit A shrinks while fading in intensity. (A small residual intensity in the interior of orbit A does not change with coverage and is attributed to indirect transitions at the bulk N point.) The shrinkage is of similar origin as the evolution of orbits 1 and 2, but in addition may also be due to charge transfer between the bulk and/or regions that have H atoms to regions that do not.

A possible electronic mechanism for the reconstruction is therefore suggested [10]: At some critical coverage θ_c, the electron orbit 1 in Fig. 1(a) contacts its equivalent orbit in the next SBZ, leading to a very long wavelength $\mathbf{q}_{||} \rightarrow 0$ electron density wave, which can be excited with little or no energy cost. This density wave is coupled to the lattice, which can relax with a rigid shift (corresponding to a phonon with $\mathbf{q}_{||} \rightarrow 0$). When the orbits merge, there is a saddle point in the band structure at E_F. Since the density of states of a saddle point diverges logarithmically, this may also play a role in strengthening the density wave's interaction with the lattice.

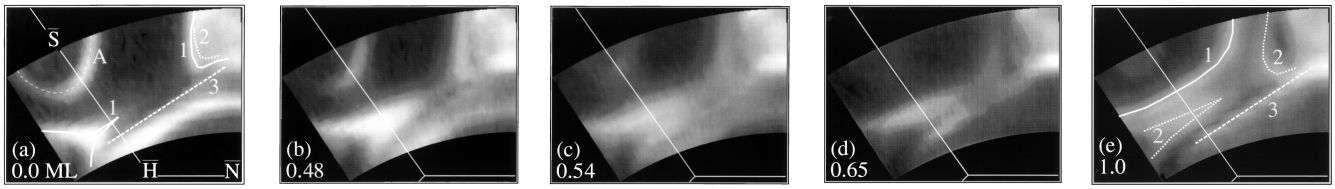

FIG. 3. Experimental Fermi contours for the wedge shown in the upper part of Fig. 1(a) as a function of hydrogen coverage from (a) clean through (e) saturated. The calibrated H coverages are indicated in ML. The white lines in (a) and (e) are guides to the eye.

There is some dispute as to whether surface reconstruction actually occurs. Calculations [4–6,21] show the surface to be shifted by amounts much less than 0.1 Å. We do not claim that the magnitude of the shift is larger than the calculated values. Rather, the shift represents a broken symmetry which, if indeed present, we propose to be related to a topological change in the Fermi contours. A recent, theoretical analysis shows that the earlier observed LEED asymmetry [11] may be completely due to non-negligible scattering from hydrogen atoms, and not underlying tungsten reconstruction [22]. A repetition of the LEED experiment for higher beam energies ($>$60 eV as used previously) for which hydrogen scattering cannot possibly play a role will settle this issue.

To summarize, we systematically measured the Fermi level crossings of W(110) as a function of hydrogen coverage from 0 to 1 ML. We concluded that two important structural properties, namely, the rigid-shift surface reconstruction proposed at 0.5 ML coverage and the Kohn anomalies observed near 1 ML, are consistent with electron-phonon coupling at $\mathbf{q}_{||} = 0$ and $\mathbf{q}_{||} = \mathbf{Q}_{c1}$ and $\mathbf{Q}_{c2}$, respectively. Current theoretical calculations, which omit spin-orbit coupling, are unable to predict a second surface state present for all coverages of hydrogen, which was key to our interpretation of the Kohn anomalies. While our measurements also hint at a mechanism for shifted-layer reconstruction, much more theoretical work is needed.

We acknowledge discussions with P. Ruggerone and J. W. Chung, and experimental assistance by K. H. Jeong and J. D. Denlinger. This work was supported by the Department of Energy, and performed at the Advanced Light Source. This work was supported by the Director, Office of Energy Research, Office of Basic Energy Science, Materials Sciences Division, of the U.S. Department of Energy, under Contract No. DE-AC03-76SF00098.

*Mailing address: MS 2-400, Lawrence Berkeley National Laboratory, Berkeley, CA 94720.

[1] E. Hulpke and J. Lüdecke, Phys. Rev. Lett. **68**, 2846 (1992).
[2] M. Balden, S. Lehwald, E. Preuss, and H. Ibach, Surf. Sci. **307**, 1141 (1994).
[3] M. Balden, S. Lehwald, and H. Ibach, Phys. Rev. B **53**, 7479 (1996).
[4] C. Bungaro, Ph.D. thesis, Scuola Internazionale Superiore di Studi Avanzati, 1995.
[5] C. Bungaro, S. d. Gironcoli, and S. Baroni, Phys. Rev. Lett. **77**, 2491 (1996).
[6] B. Kohler, P. Ruggerone, M. Scheffler, and E. Tosatti, Z. Phys. Chem. **197**, 193 (1996).
[7] B. Kohler, P. Ruggerone, and M. Scheffler, Phys. Rev. B **56**, 13 503 (1997).
[8] M. Y. Chou (private communication).
[9] G. A. Toombs, Phys. Rep. **40**, 181 (1978).
[10] R. H. Gaylord, K. H. Jeong, and S. D. Kevan, Phys. Rev. Lett. **62**, 2036 (1989).
[11] J. W. Chung, S. C. Ying, and P. J. Estrup, Phys. Rev. Lett. **56**, 749 (1986).
[12] M. Tringides and R. Gomer, Surf. Sci. **155**, 254 (1985).
[13] D. M. Riffe, G. K. Wertheim, and P. H. Citrin, Phys. Rev. Lett. **65**, 219 (1990).
[14] V. T. Cherepin *et al.*, J. Electron Spectrosc. Relat. Phenom. **68**, 105 (1994).
[15] T. Warwick *et al.*, Rev. Sci. Instrum. **66**, 2037 (1995).
[16] F. Marsiglio, Phys. Rev. B **47**, 5419 (1993).
[17] L. F. Mattheiss and D. R. Hamann, Phys. Rev. B **29**, 5372 (1984).
[18] S. LaShell, B. A. McDougall, and E. Jensen, Phys. Rev. Lett. **77**, 3419 (1996).
[19] E. Rotenberg and S. D. Kevan (unpublished).
[20] B. Kohler, P. Ruggerone, S. Wilke, and M. Scheffler, Phys. Rev. Lett. **74**, 1387 (1995).
[21] K. W. Kwak, M. Y. Chou, and N. Troullier, Phys. Rev. B **53**, 13 734 (1996).
[22] M. Arnold *et al.*, Surf. Sci. **382**, 288 (1997).